THE JOURNAL OF BIOLOGICAL CHEMISTRY VOL. 281, NO. 31, pp. 22190–22199, August 4, 2006

A Basic Leucine Zipper Transcription Factor, G-box-binding Factor 1, Regulates Blue Light-mediated Photomorphogenic Growth in *Arabidopsis*[*]

Received for publication, February 7, 2006, and in revised form, April 24, 2006 Published, JBC Papers in Press, April 25, 2006, DOI 10.1074/jbc.M601172200

Chandrashekara Mallappa[1], **Vandana Yadav**[1], **Prem Negi, and Sudip Chattopadhyay**[2]

From the National Centre for Plant Genome Research, Laboratory 101, Aruna Asaf Ali Marg, New Delhi 110067, India

Several transcriptional regulators have been identified and demonstrated to play either positive or negative regulatory roles in seedling development. However, the regulatory coordination between hypocotyl elongation and cotyledon expansion during early seedling development in plants remains unknown. We report the identification of a Z-box binding factor (ZBF2) and its functional characterization in cryptochrome-mediated blue light signaling. *ZBF2* encodes a G-box binding factor (GBF1), which is a basic leucine zipper transcription factor. Our DNA-protein interaction studies reveal that ZBF2/GBF1 also interacts with the Z-box light-responsive element of light-regulated promoters. Genetic analyses of *gbf1* mutants and overexpression studies suggest that GBF1 acts as a repressor of blue light-mediated inhibition in hypocotyl elongation, however, it acts as a positive regulator of cotyledon expansion during photomorphogenic growth. Furthermore, whereas GBF1 acts as a positive regulator of lateral root formation, it differentially regulates the expression of light-inducible genes. Taken together, these results demonstrate that GBF1 is a unique transcriptional regulator of photomorphogenesis in blue light.

Arabidopsis seedlings are genetically defined to follow two distinct developmental pathways: skotomorphogenesis or etiolation in the dark and photomorphogenesis or de-etiolation in the light (1–3). In the dark, seedlings grow with elongated hypocotyls, small and closed cotyledons, and the light-inducible genes are expressed either at low or below detectable levels. The presence of light inhibits hypocotyl elongation, promotes cotyledon opening and expansion, and thus results in photomorphogenesis. The light-inducible genes are expressed at high levels during photomorphogenic growth.

Plants are able to perceive various wavelengths of light through photoreceptors. Far-red and red light are perceived by phytochromes (phyA to phyE)[3]; whereas cryptochromes (cry1 and cry2) are involved in the perception of blue and UV-A light (4–7). Recent studies have made significant progress in the identification and functional characterization of downstream components in phytochrome signaling (1, 2, 6–8). HYH, AtPP7, and ZBF1/MYC2 have been reported as blue light (BL)-specific regulators of photomorphogenic growth in *Arabidopsis* (9–11). However, the connection of photoperception to transcription in BL still remains largely unclear (11).

Several transcription factors have been reported that are involved in early seedling development in *Arabidopsis* (11–22). COP1, a repressor of photomorphogenesis in the dark, acts as an ubiquitin ligase, and it interacts with and mediates the degradation of photomorphogenesis promoting factors such as HY5, HYH, LAF1, and HFR1 in the dark (9, 23–26). Recent studies have shown that COP1 interacts with SPA1, a negative regulator acting in far-red light, and this interaction is critical for proteasome-mediated degradation of HY5 and LAF1 (25, 27, 28).

Analyses of the promoter sequences of light-inducible genes, including *CAB*, *RBCS*, and *CHS*, have led to identification of at least four commonly found light-responsive elements (LREs): G, GATA, GT1, and Z-box, which have been demonstrated to be essential for light-mediated transcriptional activity (29–35). Several LRE-specific transacting factors have been identified earlier, and in some cases the genes that encode such factors have been cloned and their functions have been investigated (31, 36). A four-member gene family encoding proteins containing basic leucine zipper DNA binding domains (GBFs) have been reported (37, 38). Extensive DNA-protein interaction studies were carried out with GBFs. The light-regulated modification and subcellular localization of GBFs have also been investigated. It has been proposed from these studies that the limited nuclear access may be an important controller of the activities of GBFs (39). However, the *in vivo* functions of these genes are yet to be defined.

A Z-DNA-forming sequence (ATACGTGT) is present in *CAB1* minimal promoter that is essential for light-dependent developmental expression of *CAB1* gene (29). Recent studies have revealed that the Z-box containing synthetic and native promoters are responsive to phyA, phyB, and cry1 photoreceptors and are under the control of downstream regulatory com-

* This work was supported by a grant from Department of Science and Technology, the Government of India, and an internal grant from National Centre for Plant Genome Research (to S. C.). The costs of publication of this article were defrayed in part by the payment of page charges. This article must therefore be hereby marked "*advertisement*" in accordance with 18 U.S.C. Section 1734 solely to indicate this fact.

The nucleotide sequence(s) reported in this paper has been submitted to the GenBank™/EBI Data Bank with accession number(s) AJ843257.

[1] Recipients of Council of Scientific and Industrial Research fellowships from the Government of India.

[2] To whom correspondence should be addressed. Tel.: 91-11-2617-8614; Fax: 91-11-2671-6658; E-mail: sudipchatto@yahoo.com.

[3] The abbreviations used are: phyA, -E, phytochromes A to E; cry1, -2, cryptochromes 1 and 2; GBF1, G-box binding factor 1; ZBF2, Z-box binding factor 2; bZIP, basic leucine zipper; LRE, light-responsive elements; GST, glutathione *S*-transferase; WL, white light; D, dark/darkness; FR, far-red light; RL, red light; BL, blue light; OE1, -2, over-expressers 1 and 2; Ler, Landsberg erecta; Col, Columbia; RLD, Reschiev; GUS, β-glucuronidase.

ponents such as COP1 and HY5 (33, 35). To identify and clone ZBFs (Z-box binding factors), we have carried out DNA-ligand binding screening to screen an *Arabidopsis* cDNA expression library and have identified several such factors. One of these ZBFs, ZBF1/MYC2, has very recently been shown to be a negative regulator of blue light-mediated photomorphogenic growth. Furthermore, it has been demonstrated that ZBF1/MYC2 acts as a point of cross-talk among light, abscisic acid, and jasmonic acid signaling pathways (11, 40, 41). We have investigated the functional relevance to light-regulated gene expression and photomorphogenic growth of another ZBF (ZBF2/GBF1) in this study.

EXPERIMENTAL PROCEDURES

Plant Materials and Transformations—Surface-sterilized seeds were sown on Murashige and Skoog plates, kept at 4 °C in darkness for 3–5 days, and transferred to light at 22 °C. The intensities of continuous light sources used in this study are: white light (100, 60, 30, 15, 5, and 1 μmol m^{-2} s^{-1}); blue light (40, 30, 15, 5, and 1 μmol m^{-2} s^{-1}); red light (95, 30, 15, and 5 μmol m^{-2} s^{-1}); and far-red light (90, 30, 15, and 5 μmol m^{-2} s^{-1}). Unless otherwise mentioned, the highest light intensities were used for the experiments.

The T-DNA-tagged mutant lines heterozygous or homozygous for the *zbf2*/*gbf1* mutations were identified by genomic PCR analyses. Individual plants of T2 generation, obtained from a self-fertilized heterozygous plant, were examined by genomic PCR using the left border-specific primer LBP: 5′-GCGTGGACCGCTTGCTGCACCT-3′ and *GBF1*-specific primers LP13: 5′-GTGCCATAAGGCGGCATCATA-3′ and RP13: 5′-TGCAAACAAACACCTTTGCATGT-3′ (for *gbf1-1* mutants); and LP14: 5′-GCACCGAACCTTGGATTTCAC-3′ and RP14: 5′-TTCCCATCCCCAGTTGGATCT-3′ (for *gbf1-2* mutants). A segregated wild-type (Col) line was used to compare the phenotypic and molecular differences with the *gbf1* mutants.

For the generation of GBF1/ZBF2 over-expresser transgenic lines, a 1.15-kb fragment of *GBF1* cDNA was PCR-amplified using primers 5′-GAAGATCTTGAGTAACACAAGTAAGTAGTAAGC-3′ and 5′-GACTAGTAATCGTAGCTTTTGCAGCTT-3′. The PCR product was digested and cloned into BglII and SpeI site of pCAMBIA1303, a binary vector carrying the cauliflower mosaic virus (CaMV) 35 S promoter. For the complementation test, a genomic fragment containing full-length *GBF1* and ~1.3 kb upstream DNA sequence was cloned into the SmaI site of pBI101.2 vector. The *Agrobacterium* strain *GV3101* was transformed individually with each recombinant construct. The *Arabidopsis* wild-type (Ws) plants (for overexpression) or *gbf1-1* mutant plants (for complementation) were transformed using *Agrobacterium*-mediated vacuum infiltration method. Transgenic plants (T1) were screened on 15 μg/ml hygromycin or 20 μg/ml kanamycin containing Murashige and Skoog plates. Several individual lines with a single T-DNA locus, as determined by the segregation of hygromycin- or kanamycin-resistant *versus* -sensitive ratios (3:1), were selected, and homozygous transgenic plants were generated for further studies.

For the generation of *gbf1 cry1*, *gbf1 cry2*, and *gbf1 phyA* double mutants, homozygous *gbf1-1* mutant plants (Col) were crossed individually with *hy4–2.23N* (Ler (4)), *cry2–1* (Col (42)), and *phyA-101* (RLD (43)) homozygous mutant lines. F2 seedlings were grown in white light (WL, 60 μmol m^{-2} s^{-1}) or far-red light (FR, 30 μmol m^{-2} s^{-1}) for the identification of *cry1*, *cry2*, or *phyA* homozygous lines, respectively, and elongated seedlings were transferred to soil. To determine the genotype at *GBF1* locus, ~40 seedlings from each line were tested by genomic PCR. F3 progeny that are homozygous for *gbf1-1* mutant plants were further tested and designated as *gbf1 cry1*, *gbf1 cry2*, and *gbf1 phyA* double mutants. Because *gbf1*, *cry1*, *cry2*, and *phyA* were of different ecotype backgrounds, F2 seedlings, which were heterozygous for *cry1*, *cry2*, or *phyA* mutations but homozygous wild type for *GBF1* were used as control (WT).

Transgenic Lines with Promoter-GUS Constructs and GUS Assays— The promoter-reporter constructs used in this study have been described (33, 35). GUS staining (using 20–30 seedlings in each sample) and GUS activity measurements (40–50 seedlings) has been described previously (34). Wild-type and *gbf1* mutant plants containing the same transgene were stained for the same length of time.

Measurements of Epidermal Cell Length and Expansion—Measurements of epidermal cell length and expansion of 6-day-old seedlings were essentially carried out as described (44, 45).

Electrophoretic Mobility Shift (Gel Shift) Assays—The full-length *GBF1* cDNA was cloned in pGEX4T-2 vector, and *GST-GBF1* was induced using 1 mM isopropyl 1-thio-β-D-galactopyranoside and overexpressed in *Escherichia coli*. The overexpressed GST-GBF1 was affinity-purified following the manufacturer's protocol (Amersham Biosciences). The DNA binding assays were performed as described (13). The 189-bp DNA fragment of *CAB1* minimal promoter was cloned into pBluescript vector after PCR with primers: forward, 5′-CGGAATTCATAAGGATAGAGAGATCTATTC-3′ and reverse, 5′-CGGGATCCTGAGGTTGCTATTGGCTAGTCAT-3′ using genomic DNA as template. The 189-bp fragment was digested with EcoRI plus BamHI, purified, and 3′-end-labeled for using as probe for the DNA binding assays. One nanogram of labeled DNA was used for each binding reactions.

Northern and Immunoblot Analyses—Total RNA was extracted using the RNeasy plant minikit (Qiagen) following the manufacturer's instruction. We used a 1.15-kb full-length cDNA fragment of GBF1 for probe preparation using random priming kit (Megaprime™, Amersham Biosciences) following the manufacturer's instructions. The DNA fragments of *CAB*, *RBCS*, and *CHS* genes were used for probes as described (11). To quantify the Northern blot data, the intensity of each band was quantified by Fluor-S-MultiImager (Bio-Rad) and ratios of the genes *GBF1*, *CAB*, *RBCS*, or *CHS versus* its corresponding 18 S rRNA band were determined and plotted.

Protein extracts were prepared from wild-type or *gbf1* mutant seedlings. 20 μg of total protein was used for immunoblot analysis. Proteins were separated by 8% SDS-PAGE. Pre-stained protein markers (Amersham Biosciences) were used for molecular mass determination. The gel was stained with Coomassie Brilliant Blue R-250 for visualization. For

immunoblot analysis, the proteins were transferred to Hybond C-Extra (Amersham Biosciences), blocked with 5% bovine serum albumin in phosphate-buffered saline (10 mM Na_2HPO_4, 1.8 mM KH_2PO_4, 140 mM NaCl, 2.7 mM KCl) and probed with affinity-purified GBF1 polyclonal antibodies.

Chlorophyll and Anthocyanin Measurements—Chlorophyll and anthocyanin contents were measured following essentially the same protocols as described in (9). Sequence data (GBF1) from this article have been deposited with the EMBL/GenBank™ data libraries under accession number AJ843257.

RESULTS

Molecular Cloning of GBF1—We screened a cDNA expression library by DNA-ligand binding screening for the identification of ZBFs. Several genes were identified and cloned from this screen, the products of which showed specific interactions with the Z-box (11, 35). We chose one of these genes, *ZBF2* (Z-box binding factor *2*), which was represented by three independent cDNA clones, for this study. One of the cDNAs of *ZBF2* isolated from the ligand binding screen appeared to be a full-length cDNA (At1g36730). It codes for a protein of 315 amino acids with a basic leucine zipper (bZIP) DNA binding domain. The same protein was earlier shown to be interacting with the G-box and designated as GBF1 (37). Therefore, hence onwards we designate this gene as *GBF1*.

GBF1 Interacts with the Z- and G-box LREs of Light-regulated Promoters—To further examine whether GBF1 was able to specifically interact with the Z-box, we purified GST-GBF1 fusion protein from *E. coli* and performed electrophoretic mobility shift (gel shift) assays using the Z-box DNA as probe. A high affinity DNA-protein complex was detected along with the free probe as shown in Fig. 1*A* (*lane 3*). This DNA binding activity of GBF1 was efficiently competed by 50 or 100 molar excess unlabeled Z-box DNA (Fig. 1*A*, *lanes 4* and *5*). Because it was earlier reported that GBF1 could interact with the G-box (Schindler *et al.* (37)), we also competed this binding activity with a consensus G-box (13). As shown in Fig. 1*A* (*lanes 6* and 7), the G-box was able to compete more efficiently this binding activity. Whereas 50 molar excess of Z-box was unable to complete the interaction completely, the unlabeled G-box was able to do so at the same molar excess. However, GT1 failed to compete for the GBF1 binding activity even at 100 M excess (Fig. 1*A*, *lane 8*).

To further test the relative affinity of GBF1 for the G- and Z-box LREs, we carried out similar experiments using the tetrameric G-box as probe. As shown in Fig. 1*B*, whereas 50 molar excess of unlabeled Z-box was unable to compete the binding activity completely, the G-box was able to efficiently compete the interaction at the same molar excess (*lanes 4–7*). In fact, further experiments using various amounts of unlabeled G- or Z-box revealed that, whereas 40 molar excess of unlabeled G-box was able to compete the binding activity, ~70 molar excess of Z-box was required to compete the binding activity of GBF1 completely (data not shown). Taken together, these results suggest that GBF1 interacts with the Z- and G-box LREs, and the protein may have slightly more affinity toward the G-box as compare with the Z-box.

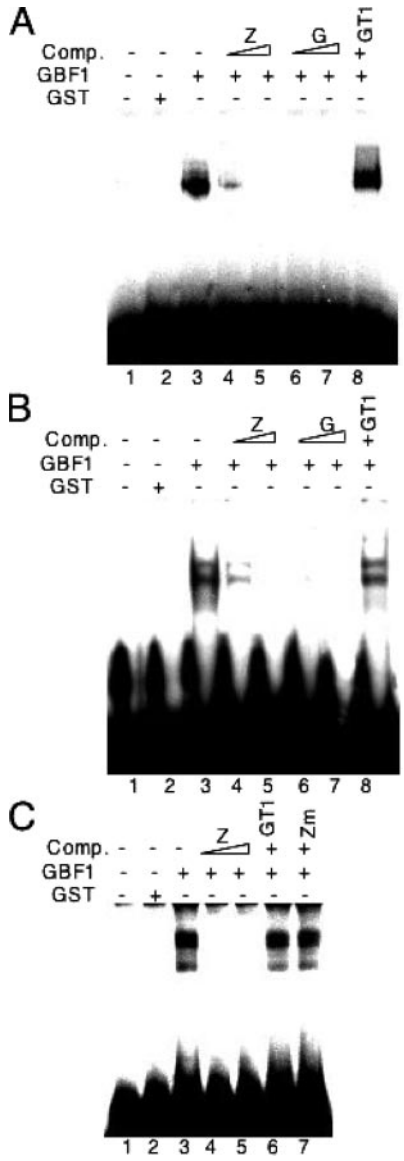

FIGURE 1. **GBF1 interacts with the Z- and G-box of light-responsive promoters.** *A*, electrophoretic mobility shift assays (gel shift) using GST-GBF1 (*GBF1*) and the consensus dimeric Z-box LRE (35) as probe. Approximately 200 ng of recombinant protein was added (*lanes 3–8*) to the radioactively labeled Z-box. No protein was added in *lane 1*, and 500 ng of GST protein was added in *lane 2*. The protein-DNA complexes were resolved on 7% native polyacrylamide gel. The *triangle* indicates increasing concentrations of the competitors (*Comp*) and the *plus* and *minus signs* indicate the presence or absence of competitors, respectively. *B*, gel-shift assays using GST-GBF1 and the consensus tetrameric G-box (13) as probe. Experimental details are as in *A*. *C*, gel-shift assays using GST-GBF1 and the native *CAB1* minimal promoter as probe. Approximately 200 ng of recombinant protein was added (*lanes 3–7*) to radioactively labeled *CAB1* DNA fragment. Experimental details are as in *A*.

To further substantiate the interaction of GBF1 with the Z-box, we tested the ability of GBF1 to interact with the Z-box present in native *CAB1* minimal promoter. The Z-box present within the minimal promoter region of *CAB1* has been shown to be critical for light regulated expression of this gene (29). The 189-bp DNA fragment of *CAB1* was used for gel shift assays. As shown in Fig. 1*C*, whereas GST alone did not show any binding activity, a strong low mobility DNA-protein complex was formed with GST-GBF1 fusion protein (*lanes 2* and *3*). This interaction was efficiently competed out with 80 or

120 molar excess of unlabeled Z-box (Fig. 1*C*, *lanes 4* and *5*) but not with 120 molar excess of GT1 or Zm, a mutated version of the Z-box (Fig. 1*C*, *lanes 6* and *7*). Taken together, these results demonstrate that GBF1 specifically binds to the Z-box of native *CAB1* minimal promoter.

Isolation and Characterization of Null Mutations in GBF1—To investigate the *in vivo* function of GBF1, we searched for mutants in T-DNA knock-out collections (46). Two independent mutant lines with T-DNA insertion were identified, and the corresponding alleles were designated as *gbf1-1* (*zbf2-1*) and *gbf1-2* (*zbf2–2*). We performed PCR genotyping analyses to determine plants that are homozygous or heterozygous for *gbf1-1* or *gbf1-2* mutations. We monitored the segregation of self-fertilized plants heterozygous for *gbf1-1* or *gbf1-2*. The segregation ratios determined by the analyses of genotyping PCR in T2 progeny suggested that a single T-DNA locus was present in each of *gbf1-1* or *gbf1-2* mutant lines. The junctions of T-DNA and *GBF1* were amplified by PCR, and the DNA sequence analyses revealed that the T-DNA was inserted in nucleotide position 80 bp upstream to the start codon of *GBF1* in *gbf1-1*, and in nucleotide position 660 bp downstream to the start codon of *GBF1* in *gbf1-2* mutants (Fig. 2*A*). Northern and immunoblot analyses were unable to detect any GBF1 mRNA or protein in *gbf1-1* or *gbf1-2* mutant backgrounds suggesting that *gbf1-1* and *gbf1-2* are likely to be null mutants (Fig. 2, *B–D*).

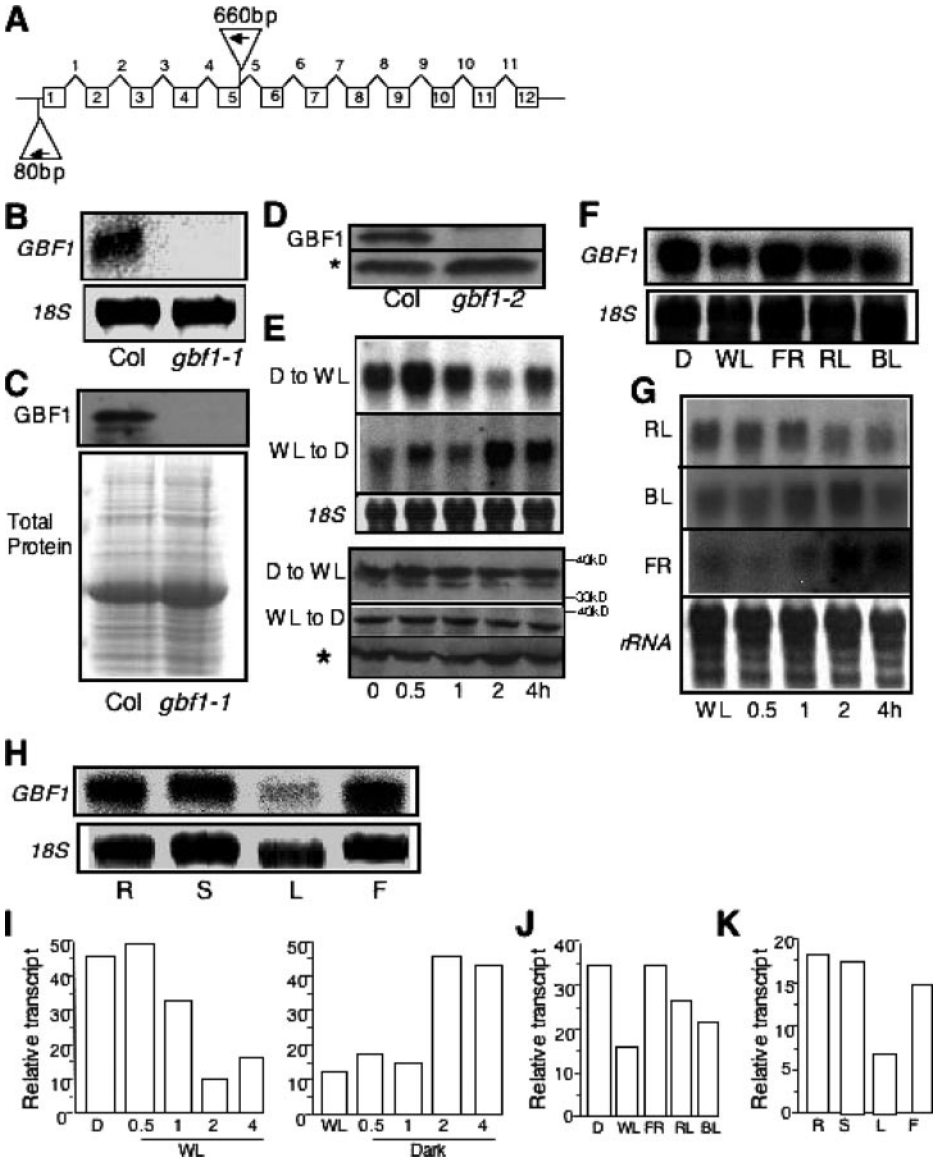

FIGURE 2. **The identification of *gbf1* mutants and the expression of *GBF1* in wild-type seedlings.** *A*, the schematic diagram of the T-DNA insertion sites in *GBF1*. The *inverted triangles* show the T-DNA insertion sites. The exons and introns are shown as *boxes* and *arrowheads*, respectively. *B*, RNA gel blot analysis of *GBF1* in segregated wild-type (Col) and *gbf1-1* mutant (Col) seedlings. 20 μg of total RNA was loaded onto each lane. The 1.15-kb full-length cDNA fragment of *GBF1* was used as probe. The 18 S rRNA is shown as loading control. *C*, immunoblot of 20 μg of total protein prepared from wild-type (Col) and *gbf1-1* mutants. Affinity-purified GBF1 polyclonal antibodies were used as primary antibody for detection of GBF1. Coomassie-stained protein gel (*Total protein*) is shown as loading control. *D*, immunoblot of 20 μg of total protein prepared from wild-type (Col) and *gbf1-2* mutants (Col). Affinity-purified GBF1 polyclonal antibodies were used as primary antibody for detection of GBF1. The *asterisk* marks a cross-reacting protein band in the same blot indicating the loading control. *E*, time course of *GBF1* transcript or protein accumulation. *Upper panel*: 5-day-old seedlings (Col) grown in constant darkness (*D*) or white light (*WL*) were transferred to WL or D, respectively, for 0.5, 1, 2, or 4 h. *GBF1* transcript of 5-day-old seedlings grown in constant D or WL are shown as 0 h. Experimental details are as in *B*. *Lower panel*: time-course experiment of GBF1 protein accumulation. Experimental details are the same as in *B* (*upper panel*) and *D*. *F*, light-regulated expression of *GBF1*. 6-day-old wild-type (Col) seedlings grown in constant darkness (*D*), WL, FR, RL, or BL were used for RNA gel blot analyses. Experimental details are the same as in *B*. *G*, expression of *GBF1* in different light qualities after WL pretreatment. 5-day-old seedlings grown in constant WL were transferred to RL, BL, or FR for 0.5, 1, 2, or 4 h, and the steady-state mRNA levels of *GBF1* were determined. Experimental details are the same as in *B*. rRNA has been shown as loading control. *H*, tissue-specific expression of *GBF1*. Total RNA was isolated from root (*R*), stem (*S*), leaf (*L*), or flower (*F*) of 30-day-old wild-type *Arabidopsis* plants grown in WL (16-h light and 8-h dark cycle). Experimental details are the same as in *B*. *I–K*, quantification of the Northern blot data in *E* (*upper panel*), *F*, and *H*, respectively, by Fluor-S-MultiImager (Bio-Rad)

Previous studies revealed that *GBF1* mRNA was present in both light and dark grown cotyledons of 5-day-old wild-type seedlings (37). To quantify and expand our understanding about the pattern of expression of *GBF1* in wild-type background, we carried out time-course experiments. For these experiments, 5-day-old seedlings grown in constant darkness or WL were transferred to WL or darkness, respectively, for 0.5, 1, 2, or 4 h, and the steady-state mRNA levels were measured. About 3-fold reduction in the expression of *GBF1* was detected after 4 h of exposure to WL as compared with dark grown seedlings (Fig. 2*E*, *upper panel* and *I*). In agreement with this observation, the expression of *GBF1*

was increased to ~4-fold after 4 h of exposure to darkness as compared with WL grown seedlings (Fig. 2*E*, *upper panel* and *I*). We performed similar time-course experiments to determine whether the level of GBF1 protein was also higher in dark grown seedlings. However, we could not detect any significant change at the protein level during dark to WL transitions or *vice versa* (Fig. 2*E*, *lower panel*). These results suggest that, although the transcript level of *GBF1* varies depending on the presence or absence of WL, the protein level remains largely unaltered.

Because *GBF1* is expressed in WL, we asked whether it was expressed under various wavelengths of light, including far-red light (FR), red light (RL), and blue light (BL). As shown in Fig. 2 (*F* and *J*), *GBF1* was expressed in all light conditions tested with maximum level of expression in FR. To further examine the light-dependent expression of *GBF1*, we carried out time-course experiments. For these experiments, 5-day-old seedlings grown in constant WL were transferred to various wavelengths of light for 0.5, 1, 2, or 4 h, and the steady-state mRNA levels of *GBF1* were determined. As shown in Fig. 2*G*, the expression of *GBF1* slightly decreased or increased in RL or BL, respectively, however the expression of *GBF1* was significantly elevated after 4 h of exposure to FR. The examination of tissue specific expression of *GBF1* in adult plants revealed that the gene was expressed in root, stem, and flower at similar levels, however ~2-fold less expression was detected in the leaf tissues (Fig. 2, *H* and *K*).

gbf1 Mutants Exhibit Blue Light-specific Morphological Defects in Seedling Development—We monitored the growth of 6-day-old *gbf1* mutant seedlings in constant darkness or WL conditions. As shown in Figs. 3*A* and 4 (*A* and *B*), no morphological difference was detected between wild-type and *gbf1* mutants grown in constant darkness. However, *gbf1* mutants displayed increased sensitivity to WL irradiation under various fluences and therefore, resulted in strikingly shorter hypocotyls as compared with the wild-type seedlings (Figs. 3*B*, 3*C*, 3*J*, and 4*A*). The effects appeared to be more pronounced within 5–30 μmol m^{-2} s^{-1} fluence rates of WL. We asked whether the hypersensitive phenotype of *gbf1* was specific to a particular wavelength of light. To address this question, the growth of 6-day-old seedlings under various wavelengths of light was tested. The enhanced inhibition in hypocotyl elongation in *gbf1* was observed in constant BL, however, no significant change in hypocotyl length was observed in constant RL or FR under various fluences (Figs. 3*D*, 3*E*, 3*F*, 3*K*, and 4*B*). Furthermore, although the hypocotyls of *gbf1* displayed hypersensitivity to WL and BL, the cotyledons were found to be less sensitive to WL and BL. Thereby, the cotyledons of *gbf1* mutants were found to be significantly smaller as compared with wild-type seedlings under WL and BL grown conditions (Figs. 3*G*, 3*H*, 3*L*, 4*C*, and 4*D*). Taken together, these results suggest that GBF1 acts as a negative regulator of inhibition of hypocotyl elongation, however, it functions as a positive regulator of cotyledon expansion in BL. The examination of the leaf size of wild-type and *gbf1* mutant plants, however, revealed no significant differences (Fig. 3*R*). A genomic fragment containing *GBF1* and its upstream sequence of ~1.3 kb was introduced into the *gbf1-1* mutants plants for complementation test. The transgenic seedlings were unable to display BL-specific phenotypes suggesting that the observed phenotypes of *gbf1* mutants are due to the loss of *GBF1* functions (data not shown).

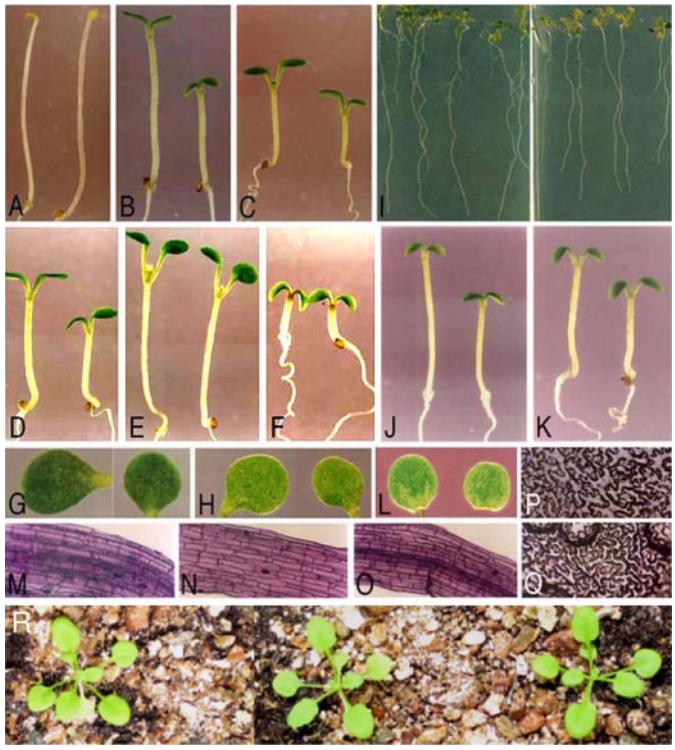

FIGURE 3. **Mutation in *GBF1* results in various effects.** Segregated wild-type (Col) and *gbf1-1* (Col) mutants (*A–I*) or *gbf1-2* (Col) mutants (*J–L*) are shown on the *left* and *right*, respectively. *A–F*, 6-day-old seedlings were grown in constant darkness, WL (5 μmol m^{-2} s^{-1}), WL (30 μmol m^{-2} s^{-1}), BL (30 μmol m^{-2} s^{-1}), RL (95 μmol m^{-2} s^{-1}), or FR (90 μmol m^{-2} s^{-1}), respectively. *G* and *H*, cotyledons of 6-day-old seedlings grown in constant WL (30 μmol m^{-2} s^{-1}), or BL (30 μmol m^{-2} s^{-1}), respectively. *I*, 16-day-old plants grown in constant WL (100 μmol m^{-2} s^{-1}). *J–K*, 6-day-old seedlings were grown in constant WL (5 μmol m^{-2} s^{-1}), or BL (30 μmol m^{-2} s^{-1}), respectively. *L*, cotyledons of 6-day-old seedlings grown in constant BL (30 μmol m^{-2} s^{-1}). *M–O*, hypocotyl epidermal cells of 6-day-old wild-type, *gbf1-1*, and *gbf1-2* seedlings, respectively, grown in constant BL (30 μmol m^{-2} s^{-1}). *P* and *Q*, imprints of cotyledon epidermal cells of 6-day-old wild-type and *gbf1-1* seedlings, respectively, grown in constant BL (30 μmol m^{-2} s^{-1}). *R*, 16-day-old wild-type, *gbf1-1*, and *gbf1-2* (from *left* to *right*) plants grown in WL (30 μmol m^{-2} s^{-1}).

To determine whether the enhanced inhibition in hypocotyl elongation or smaller cotyledon size of *gbf1*mutants is due to the altered cell elongation or expansion, we examined the size of epidermal cells of *gbf1* mutants and compared with the wild-type 6-day-old seedlings grown in BL. As shown in Figs. 3 (*M–O*) and 6*B*, the epidermal cells of hypocotyls were significantly shorter in *gbf1* mutants as compared with the wild type. Similarly, the epidermal cells of cotyledons were found to be significantly less expanded in *gbf1* mutants as compared with 6-day-old wild-type seedlings (Fig. 3, *P* and *Q*). These results indicate that GBF1 acts as a regulator of growth that promotes cell elongation and expansion and thus the loss of *GBF1* function mutants result in shorter hypocotyls and less expanded cotyledons during seedling development.

To investigate whether *gbf1* mutants have any additional morphological defects, we examined and compared the root growth of *gbf1* mutants with wild-type plants. The *gbf1* mutant

plants produced significantly less number of lateral roots as compared with wild-type plants suggesting that GBF1 is essential for optimum lateral root formation (Figs. 3*I* and 6*D*).

While propagating *gbf1* mutant plants, we observed that the *gbf1* mutation caused early flowering. Whereas long-day-grown (16-h light/8-h dark cycles) wild-type plants start flowering after the formation of ~10–11 rosette leaves, *gbf1* mutants flower after producing ~7–8 rosette leaves (Fig. 6, *A* and C). However, such effect was not detected in short-day-grown (8-h light/16-h dark cycles) *gbf1* mutant plants (data not shown).

Mutations in GBF1 Result in Altered Chlorophyll Accumulation—Chlorophyll and anthocyanin syntheses are two important physiological responses regulated by light. To examine whether *gbf1* mutants have altered chlorophyll or anthocyanin accumulation, we measured the chlorophyll and anthocyanin contents in *gbf1* mutant seedlings. We measured the chlorophyll content of cotyledons and normalized the chlorophyll content by cotyledon size. The chlorophyll content was found to be significantly lower in *gbf1* mutants as compared with wild-type seedlings (Fig. 4*E*). No difference in accumulation of anthocyanin was detected between wild-type and *gbf1* mutant seedlings (data not shown).

gbf1 Mutants Are Epistatic to cry1 and cry2—To determine the involvement of photoreceptors such as cry1, cry2, and phyA in BL-specific functions of GBF1, we performed epistasis analyses. We generated *gbf1 cry1*, *gbf1 cry2*, and *gbf1 phyA* double mutants and examined the hypocotyl length in comparison to *cry1* (Ler), *cry2* (Col), *phyA* (RLD), and *gbf1* (Col) mutants. Measurements of hypocotyl length revealed that double mutants such as *gbf1 cry1* and *gbf1 cry2* displayed similar hypocotyl lengths as *gbf1* mutants in BL (Fig. 4, *F* and *G*). However, *gbf1 phyA* double mutants exhibited hypocotyl length similar to *phyA* mutants in BL (Fig. 4*H*). These results suggest that GBF1 likely acts downstream to both cry1 and cry2 photoreceptors and the increased sensitivity to BL caused by the *gbf1* mutation requires blue light perception by phyA.

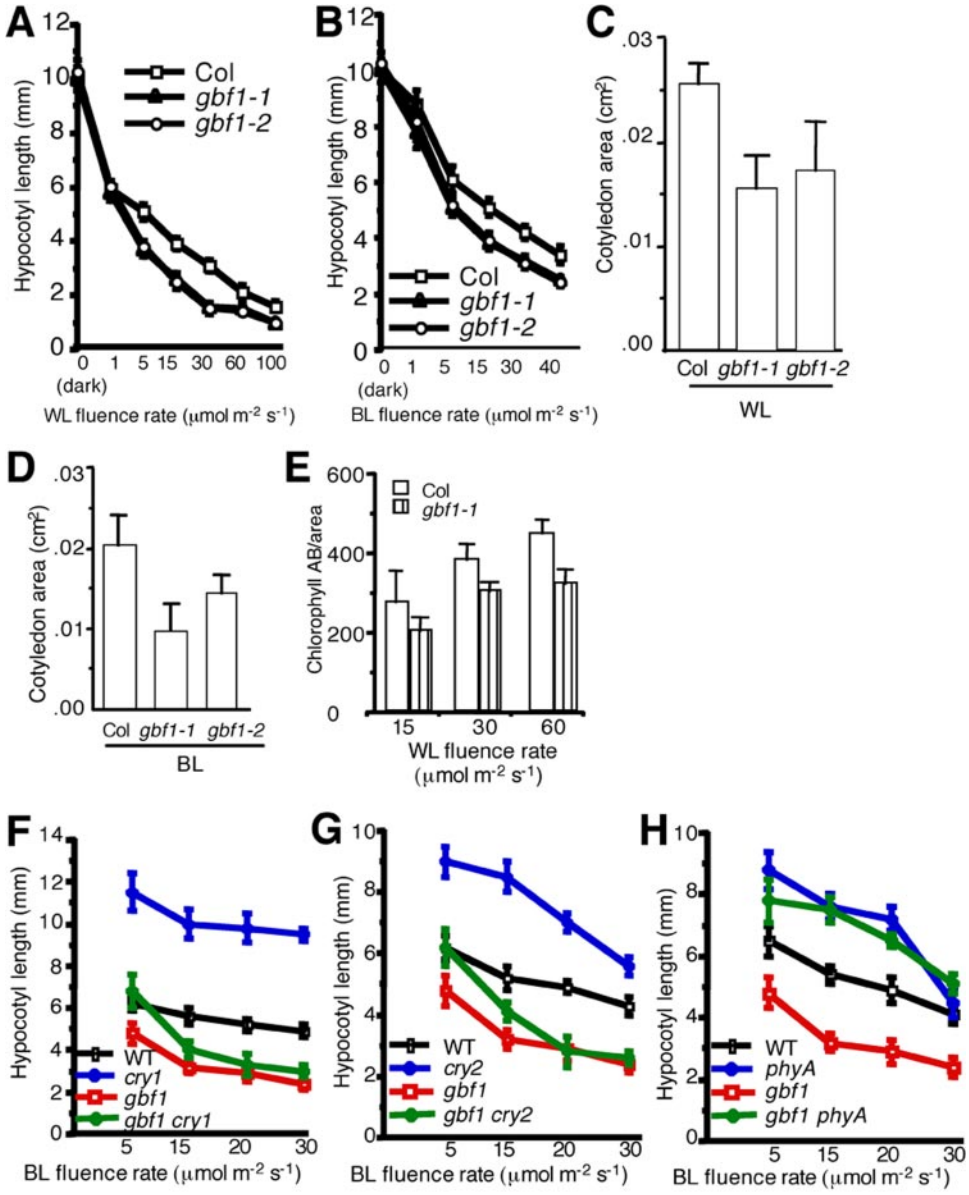

FIGURE 4. **Characterization of *gbf1* mutants.** ~25–30 seedlings were used for the measurement of hypocotyl length, cotyledon area, or chlorophyll accumulation. The *error bars* indicate standard deviations. The *gbf1* mutants are in Columbia background. *A* and *B*, quantification of hypocotyl length of 6-day-old wild-type (Col) and *gbf1* mutant seedlings grown at various fluence rates in constant WL or BL, respectively. *C* and *D*, quantification of cotyledon area of 6-day-old wild-type (Col) and *gbf1* mutant seedlings grown in constant WL (30 μmol m^{-2} s^{-1}) or BL (30 μmol m^{-2} s^{-1}), respectively. *E*, accumulation of chlorophyll a and b in the cotyledons after normalized by cotyledon size in 6-day-old wild-type (Col) and *gbf1-1* mutant seedlings. *F–H*, hypocotyl lengths of 6-day-old wild-type (WT: see "Experimental Procedures"), *gbf1*, *cry1* (Ler), *gbf1 cry1*, *cry2* (Col), *gbf1 cry2*, *phyA* (RLD), and *gbf1 phyA* seedlings grown at various fluence rates of BL.

GBF1 Over-expressers Display BL-specific Regulation of Hypocotyl and Cotyledon Growth in Opposite Manner—Because the loss of GBF1 function resulted in shorter hypocotyls and less expanded cotyledons, we asked whether higher levels of GBF1 cause opposite effects. Several independent transgenic lines expressing *GBF1* cDNA driven by CaMV 35 S promoter were generated for this study. We selected multiple transgenic lines segregating for a single T-DNA locus, determined by hygromycin resistance, for the production of homozygous lines and further analysis. Examination of photoresponsiveness revealed that the transgenic lines displayed significant reduction of inhibition in hypocotyl elongation in

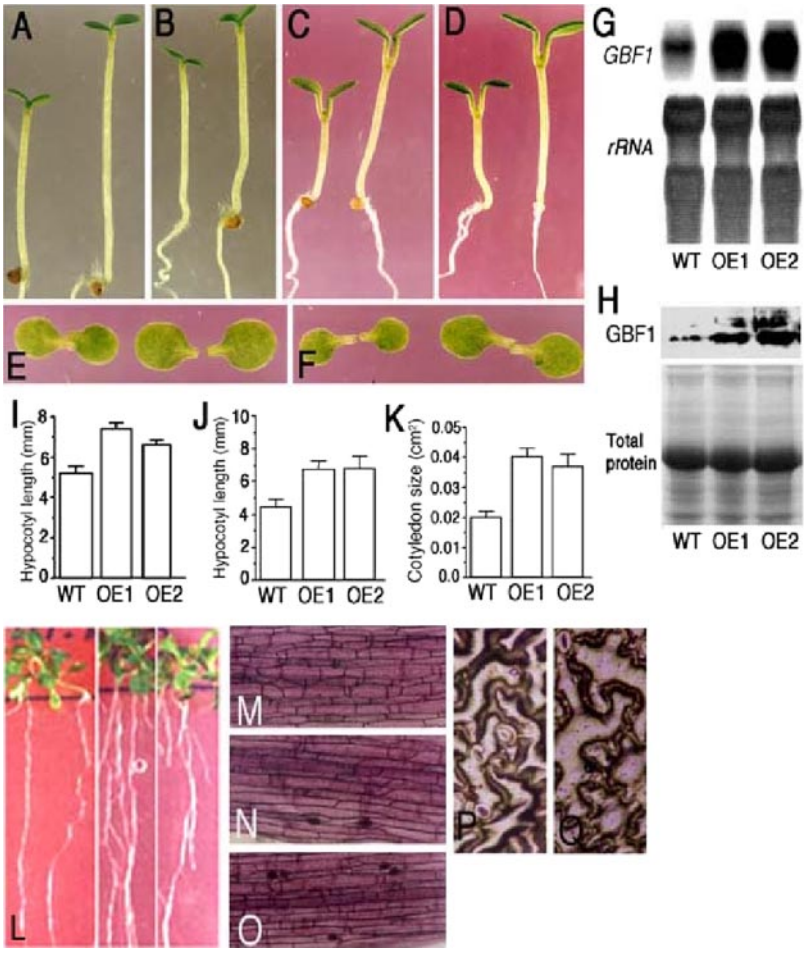

FIGURE 5. **Regulation of blue light-mediated photomorphogenic growth in GBF1 over-expresser lines.** In each panel from *A* to *F*, wild-type (Ws) and GBF1 over-expresser seedlings (OE1 or OE2 in Ws background) are shown on the *left* and *right*, respectively. *A*, 6-day-old wild-type and OE1 seedlings grown in constant WL (5 μmol m^{-2} s^{-1}); *B*, 6-day-old wild-type and OE2 seedlings grown in constant WL (5 μmol m^{-2} s^{-1}); *C*, 6-day-old wild-type and OE1 seedlings grown in constant BL (30 μmol m^{-2} s^{-1}); *D*, 6-day-old wild-type and OE2 seedlings grown in constant BL (30 μmol m^{-2} s^{-1}); *E*, cotyledons of 6-day-old wild-type and OE1 seedlings grown in constant BL (30 μmol m^{-2} s^{-1}); *F*, cotyledons of 6-day-old wild-type and OE2 seedlings grown in constant BL (30 μmol m^{-2} s^{-1}). *G*, RNA blot analysis of *GBF1* in wild-type Ws (*WT*), OE1, and OE2 seedlings. 20 μg of total RNA was loaded onto each lane. The 1.15-kb full-length cDNA fragment of *GBF1* was used as probe. rRNA is shown as loading control. *H*, immunoblot of 20 μg of total protein prepared from wild-type Ws (*WT*), OE1, and OE2 seedlings. Affinity-purified GBF1 polyclonal antibodies were used for the detection of GBF1. Coomassie-stained protein gel (*Total protein*) is shown as the loading control. *I* and *J*, quantification of hypocotyl length of 6-day-old wild-type Ws (*WT*), OE1, and OE2 seedlings grown in constant WL (5 μmol m^{-2} s^{-1}) or BL (30 μmol m^{-2} s^{-1}), respectively. About 25 seedlings were used for the measurement of hypocotyl length. The *error bars* indicate standard deviations. *K*, quantification of cotyledon area of 6-day-old wild-type Ws (*WT*), OE1, and OE2 seedlings grown in BL (30 μmol m^{-2} s^{-1}). Experimental details are the same as in *I–J*. *L*, formation of lateral roots in 16-day-old wild-type Ws, OE1, and OE2 plants (from *left* to *right*) grown in constant WL (80 μmol m^{-2} s^{-1}). *M–O*, hypocotyl epidermal cells of 6-day-old wild-type, OE1, or OE2 seedlings, respectively, grown in constant BL (30 μmol m^{-2} s^{-1}). *P* and *Q*, imprints of cotyledon epidermal cells of 6-day-old wild-type or OE1 seedlings, respectively, grown in constant BL (30 μmol m^{-2} s^{-1}).

WL and BL with no visible effect in RL or FR (Fig. 5, *A–D*, *I–J*, and data not shown). Furthermore, cotyledons of the over-expresser transgenic lines were strikingly more expanded as compared with wild-type seedlings (Fig. 5, *E*, *F*, and *K*). Determination of *GBF1* transcript and protein levels showed dramatically elevated levels of expression of this gene in over-expresser lines relative to wild-type background (Fig. 5, *G* and *H*). These results indicate that the altered phenotypes of the over-expresser lines observed were likely to be caused due to the elevated levels of GBF1.

We examined the length and size of epidermal cells of 6-day-old over-expresser and wild-type seedlings grown in BL. The epidermal cells of hypocotyls were detected to be significantly longer in GBF1 over-expresser lines as compared with wild-type seedlings (Figs. 5 (*M–O*) and 6*B*). Similarly, the epidermal cells of cotyledons were significantly more expanded in over-expresser lines as compared with wild-type seedlings (Fig. 5*P*-Q). Taken together, these results firmly demonstrate that the bZIP protein, GBF1, is a transcriptional regulator of photomorphogenic growth that promotes cell elongation and expansion during early seedling development in *Arabidopsis*.

Because the loss of function mutant *GBF1* displayed less lateral roots as compared with wild-type plants, we examined whether over-expression of GBF1 caused more lateral root formation in *Arabidopsis* plants. As shown in Figs. 5*L* and 6*D*, the over-expresser transgenic lines indeed formed more lateral roots as compared with wild-type plants suggesting that GBF1 acts as a positive regulator of lateral root formation. Examination of flowering time of the over-expresser lines revealed that *GBF1* transgenic over-expresser lines flower significantly late after formation of 15–18 rosettes as compared with wild-type plants (Fig. 6, *A* and *C*).

GBF1 Differentially Regulates the Expression of Light-inducible Genes—The up-regulation of light-inducible genes such as *CAB* and *RBCS* is one of the important phenomena in photomorphogenic growth. Because GBF1 regulates the growth of hypocotyls and cotyledons in response to BL, we asked whether the bZIP transcription factor GBF1 also plays a role in light-regulated gene expression. For this study, we used 6-day-old wild-type and *gbf1-1* mutant seedlings grown in constant dark or various light conditions and measured the relative steady-state mRNA levels of light-inducible genes. Whereas no difference in the expression of *CHS* was detected between wild-type and *gbf1* mutants, the expression of *RBCS* was found to be significantly higher in *gbf1* as compared with wild-type seedlings grown in BL or WL (Fig. 7*A*). No alteration in the expression of *CAB* was detected in WL, however, the expression of the gene was significantly reduced in BL grown seedlings (Fig. 7*A*). To further examine the BL-mediated regulation of *CAB* gene expression in

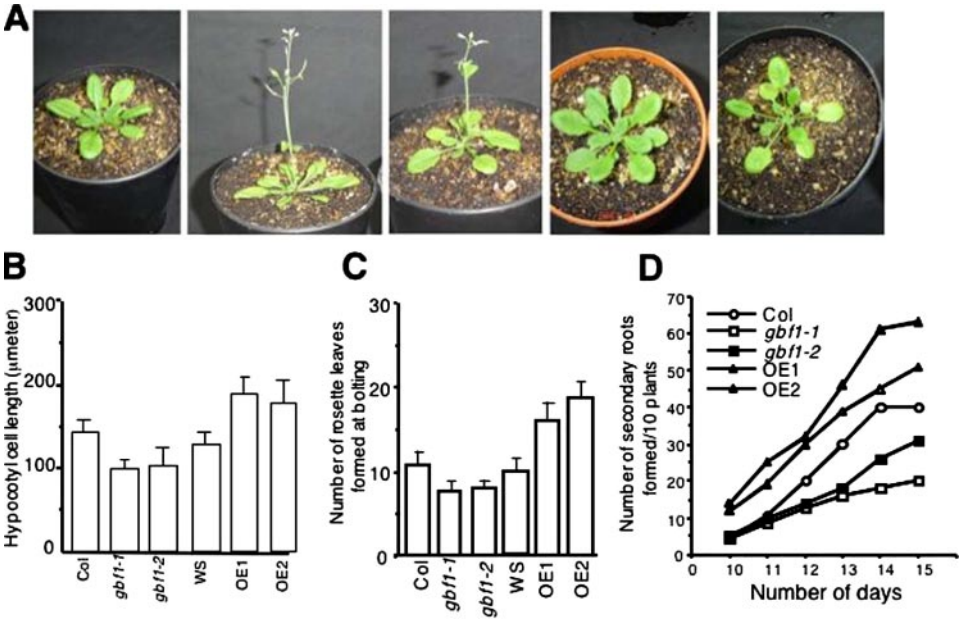

FIGURE 6. **Characterization of *GBF1* over-expresser lines.** *A*, 30-day-old wild-type (Col), *gbf1-1*, *gbf1-2*, GBF1 over-expresser 1 (OE1) and over-expresser 2 (OE2) plants (from *left* to *right*) grown in WL (80 μmol m^{-2} s^{-1}) under 16-h light/8-h dark cycles. *B*, quantification of epidermal cell lengths of hypocotyls of 6-day-old wild-type (Col), *gbf1-1*, *gbf1-2*, wild-type (Ws), OE1, and OE2 seedlings grown in constant BL (30 μmol m^{-2} s^{-1}). *C*, number of rosette leaves formed at the time of bolting in wild-type (Col), *gbf1-1*, *gbf1-2*, wild-type (Ws), OE1, and OE2 plants grown under long-day conditions of 16-h WL (80 μmol m^{-2} s^{-1}) and 8-h dark cycles. *D*, quantification of the number of lateral roots formed in wild-type (Col), *gbf1-1*, *gbf1-2*, OE1, and OE2 plants grown in constant WL (80 μmol m^{-2} s^{-1}) at various days (from day 10 to 15).

gbf1-1 mutant background, 4-day-old seedlings grown in darkness were transferred to BL for 12, 24, and 48 h, and the transcript levels were measured. Whereas >7-fold induction in *CAB* gene expression was found at 24 h in wild-type, <4-fold induction was detected in *gbf1-1* mutant background (Fig. 7, *B* and *C*), suggesting that the induction of *CAB* gene expression was significantly compromised in *gbf1-1* mutants. These results suggest that, although GBF1 negatively regulates the expression of *RBCS*, it acts as a positive regulator of *CAB* gene expression (Fig. 7*H*).

To further investigate the above observation, we used two stable transgenic lines: *Z/NOS101-GUS* and *CAB1-GUS* (33, 34). Both these promoter-reporter constructs were individually introduced into *gbf1-1* mutants by genetic crosses with wild-type transgenic lines (35). Mutant lines homozygous for each transgene were then generated for further studies. The *Z/NOS101-GUS* transgene was expressed in all the tissues in *gbf1* mutants similar to wild-type seedlings in BL (Fig. 7*D*). Quantitative GUS activity measurements revealed that there was ~50% reduction in the activity of this promoter in *gbf1* mutants as compared with wild-type background (Fig. 7*F*). The expression of *CAB1-GUS* transgene has been shown to be confined to the cotyledons in wild-type background (35). As shown in Fig. 7*E*, very little expression was detected (if any) of *CAB1-GUS* transgene in the *gbf1* mutants, and the quantification GUS activity measurements revealed that the activity of the *CAB1* promoter was reduced to ~4-fold in *gbf1* mutants as compared with the wild-type background (Fig. 7*G*). Taken together, these results strongly suggest that GBF1 is required for the proper activation of the Z-box-containing promoters in BL.

DISCUSSION

Although the GBF family of transcription factors has been known for more than a decade, the physiological functions of these genes remain elusive (37–39). Several transcription factors have been reported in light signaling that play either positive or negative regulatory roles in seedling development (9, 11, 14, 41). This study establishes GBF1 as a unique transcription factor in light signaling that plays both positive and negative regulatory roles in photomorphogenic growth and gene expression.

GBF1 Interacts with Both the G- and Z-box LREs—The DNA-protein interaction data in this study provide several lines of evidence that GBF1 interacts with both the Z- and G-box LREs of light regulated promoters. The competitive gel shift assays using several LREs, including the Z- and G-box, demonstrate that, although GBF1 interacts with both Z- and G-box, the protein may have higher affinity for the G-box as compared with the Z-box LRE. The recognition of the G- and Z-box LREs by GBF1 possibly indicates that these two LREs are functionally equivalent (11) with the context to GBF1 transcription factor.

Mutations in GBF1 Result in Multiple Effects—The analysis of seedling morphology of *gbf1* mutants demonstrates that the shorter hypocotyl phenotype is restricted to BL. Therefore, although *GBF1* is expressed at various wavelengths of light, it specifically acts as a negative regulator of BL-mediated inhibition of hypocotyl elongation. Our results further demonstrate that *gbf1* mutants have smaller cotyledons as compared with wild-type seedlings in blue light, thus demonstrating a positive regulatory function of GBF1 in cotyledon expansion in a blue light-specific manner. The results of epistasis analyses indicate that GBF1 acts downstream to both cry1 and cry2 photoreceptors, and the increased sensitivity to BL caused by *gbf1* mutation also requires light perception by phyA. Thus GBF1-mediated inhibition is likely to play an important role in negative or positive feedback control of cryptochrome signaling, although the function of phyA is likely to be independent of GBF1. Thus, GBF1 plays a dual but opposite regulatory role in early seedling development acting downstream to both cry1 and cry2 photoreceptors (Fig. 7*H*).

Overexpression of GBF1 has resulted in elongated hypocotyls but more expanded cotyledons in blue light, thereby confirming the differential regulatory role of GBF1 in cotyledon and hypocotyl growth. This finding further indicates that *GBF1* transcripts may not be present at sufficiently high

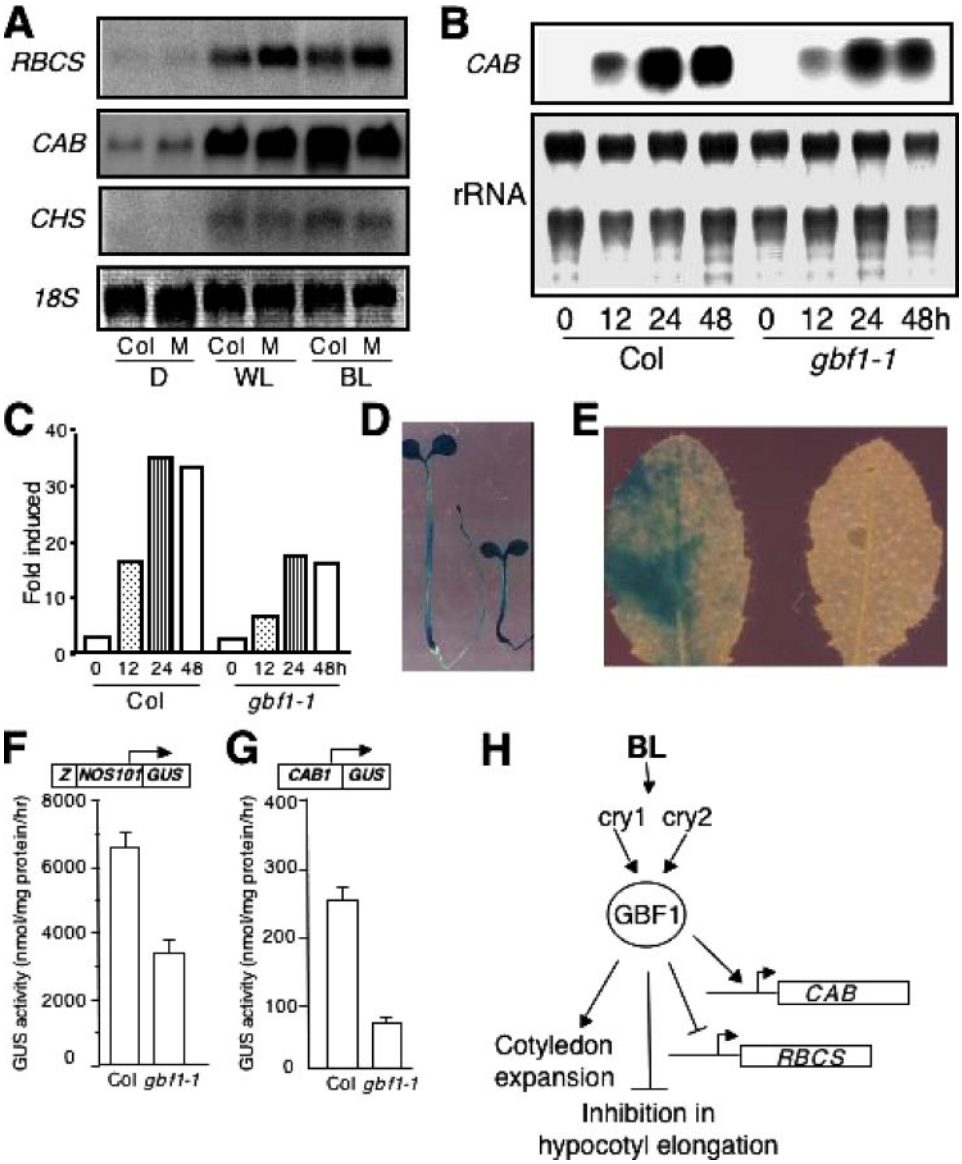

FIGURE 7. **The light-regulated gene expression in *gbf1* mutants.** *A*, RNA gel-blot analysis of *RBCS*, *CAB*, and *CHS* genes in segregated wild-type (Col) and *gbf1-1* mutant (Col) seedlings (*M*) grown in constant darkness (*D*), WL, or BL conditions. 10 μg of total RNA was loaded onto each lane. 18 S rRNA has been shown as loading control. *B*, RNA gel-blot analysis of *CAB* in segregated wild-type (Col) and *gbf1-1* mutant seedlings. 4-day-old dark grown seedlings were transferred to BL for 12, 24, or 48 h, and total RNA was extracted from each sample for RNA gel-blot analysis. 10 μg of total RNA was loaded onto each lane. 6-day-old seedlings grown in darkness are shown as 0 h. rRNA was used as loading control. *C*, quantification of the data in *B* by Fluor-S-Multilmager (Bio-Rad). *D* and *E*, 6-day-old seedlings carrying *Z/NOS101-GUS* or 12-day-old plants carrying *CAB1-GUS* transgene, respectively, were grown in BL (30 μmol m^{-2} s^{-1}) and used for GUS activity staining. In each panel wild-type (Col) and *gbf1-1* mutants (Col) are shown on the *left* and *right* side, respectively. *F* and *G*, GUS activities of 6-day-old constant BL (30 μmol m^{-2} s^{-1}) grown seedlings carrying *Z/NOS101-GUS* or *CAB1-GUS* transgenes, respectively. The *error bars* indicate standard deviations. The promoter-reporter constructs are diagrammed at the *top* of each *panel*. *H*, a working model shows BL-specific regulatory role of GBF1 during early seedling development in *Arabidopsis*.

levels in wild-type seedlings and thus may be a rate-limiting factor for cotyledon expansion in blue light signaling. However, because higher levels of GBF1 result in elongated hypocotyls, a fine controlled level of GBF1 is likely to be essential for plants to obtain blue light-mediated optimum photomorphogenic growth. This notion is further supported by the fact that GBF1 promotes cell elongation and expansion in hypocotyl and cotyledon, respectively.

HYH, AtPP7, SUB1, and MYC2/ZBF1 have been reported as downstream components in blue light signaling. Whereas SUB1, a Ca^{2+}-binding protein, functions as a negative regulator in blue and far-red light signaling, AtPP7, an Ser/Thr protein phosphatase, acts as a positive regulator of blue light-mediated photomorphogenic growth (10, 42). HYH, a transcription factor and a close homolog of HY5, acts as a positive regulator in BL signaling (9). MYC2 is a Z-box-binding transcription factor, which acts as a negative regulator in BL-mediated photomorphogenic growth and is a point of cross-talk among light, abscisic acid, and jasmonic acid signaling (11).

GBF1 Differentially Regulates the Expression of Light-inducible Genes—It has been shown that PIF3 exhibits opposite regulatory effects on seedling morphology and light-regulated gene expression in an RL- and FR-specific manner (22). Furthermore, the presence of parallel and branched pathways of light-regulated gene expression has already been suggested (17, 47, 48). Analyses of light-regulated gene expression in *gbf1* mutants have revealed that, although GBF1 is required for the proper activation of *CAB* gene expression, it acts as a negative regulator for *RBCS* gene expression (Fig. 7*H*). Transgenic studies with synthetic and native promoter-reporter constructs further indicate that GBF1 is required for the proper activation of the Z-box-containing promoters, including *CAB1*. Extensive heterodimerization of bZIP proteins has been reported (37). Thus, heterodimerization of GBF1 with other bZIP proteins could be a potential mechanism *in vivo* to generate positive and negative regulators, which in turn may play opposite roles for light-regulated gene expression and seedling development.

Acknowledgments—We thank Prof. Sushil Kumar, Dr. Shikha Bhatia, and Sreeramaiah N. Gangappa for critically reading and commenting on the manuscript.

REFERENCES

1. Deng, X. W., and Quail, P. H. (1999) *Semin. Cell Dev. Biol.* **10,** 121–129
2. Neff, M. M., Fanhauser, C., and Chory, J. (2000) *Genes Dev.* **14,** 257–271
3. Chen, M., Chory, J., and fankhauser, C. (2004) *Annu. Rev. Genet.* **38,** 87–117

4. Cashmore, A. R., Jarillo, J. A., Wu, Y. J., and Liu, D. (1999) *Science* **284,** 760–765
5. Lin, C. (2002) *Plant Cell* **14,** (suppl.) S207–S225
6. Quail, P. H. (2002) *Curr. Opin. Cell Biol.* **14,** 180–188
7. Schepens, I., Duek, P., and Fankhauser, C. (2004) *Curr. Opin. Plant Biol.* **7,** 564–569
8. Nagy, F., and Schafer, E. (2002) *Annu. Rev. Plant Biol.* **53,** 329–355
9. Holm, M., Ma, L.-G., Qn, L.-J., and Deng, X. W. (2002) *Genes Dev.* **16,** 1247–1259
10. Moller, S. G., Kim, Y.-S., Kunkel, T., and Chua, N.-H. (2003) *Plant Cell* **15,** 1111–1119
11. Yadav, V., Mallappa, C., Gangappa, S. N., Bhatia, S., and Chattopadhyay, S. (2005) *Plant Cell* **17,** 1953–1966
12. Oyama, T., Shimura, Y., and Okada, K. (1997) *Genes Dev.* **11,** 2983–2995
13. Chattopadhyay, S., Ang, L. H., Puente, P., Deng, X. W., and Wei, N. (1998) *Plant Cell* **10,** 673–683
14. Ni, M., Halliday, K. J., Tepperman, J. M., and Quail, P. H. (1998) *Cell* **95,** 657–667
15. Wang, Z.-Y., and Tobin, E. M. (1998) *Cell* **93,** 1207–1217
16. Fairchild, C. D., Schumaker, M. A., and Quail, P. H. (2000) *Genes Dev.* **14,** 2377–2391
17. Soh, M. S., Kim, Y.-M., Han, S.-J., and Song, P.-S. (2000) *Plant Cell* **12,** 2061–2073
18. Spiegelman, J. I., Mindrinos, M. N., Fankhauser, C., Richards, D., Lutes, J., Chory, J., and Oefner, P. J. (2000) *Plant Cell* **12,** 2485–2498
19. Ballesteros, M. L., Bolle, C., Lois, L. M., Moore, J. M., Vielle-Calzada, J. P., Grossniklaus, U., and Chua, N. H. (2001) *Genes Dev.* **15,** 2613–2625
20. Huq, E., and Quail, P. (2002) *EMBO J.* **21,** 2441–2450
21. Mizoguchi, T., Wheatley, K., Hanzawa, Y., Wright, L., Mizoguchi, M., Song, H. R., Carre, I. A., and Coupland, G. (2002) *Dev Cell* **2,** 629–641
22. Kim, J., Yi, H., Choi, G., Shin, B., Song, P.-S., and Choi, G. (2003) *Plant Cell* **15,** 2399–2407
23. Ang, L. H., Chattopadhyay, S., Wei, N., Oyama, T., Okada, K., Batschauer, A., and Deng, X. W. (1998) *Mol. Cell* **1,** 213–222
24. Osterlund, M. T., Hardtke, C. S., Wei, N., and Deng, X. W. (2000) *Nature* **405,** 462–466
25. Seo, H. S., Yang, J.Y., Ishikawa, M., Bole, C., Ballesteros, M. L., and Chua, N.-H. (2003) *Nature* **423,** 995–999
26. Yang, J., Lin, R., Sullivan, J., Hoecker, U., Lin, B., Xu, L., Deng, X.-W., and Wang, H. (2005) *Plant Cell* **17,** 804–821
27. Saijo, Y., Sullivan, J. A., Wang, H., Yang, J., Shen, Y., Rubio, V., Ma, L., Hoecker, U., and Deng, X.-W. (2003) *Genes Dev.* **17,** 2642–2647
28. Laubinger, S., Fittingoff, K., and Hoecker, U. (2004) *Plant Cell* **16,** 2293–2306
29. Ha, S.-B., and An, G. (1988) *Proc. Natl. Acad. Sci. U. S. A.* **85,** 8017–8021
30. Donald, R. G. K., and Cashmore, A. R. (1990) *EMBO J.* **9,** 1717–1726
31. Terzaghi, W. B., and Cashmore, A. R. (1995) *Annu. Rev. Plant Physiol. Plant Mol. Biol.* **46,** 445–474
32. Batschauer, A., Rocholl, M., Kaiser, T., Nagatani, A., Furuya, M., and Schafer, E. (1996) *Plant J* **9,** 63–69
33. Puente, P., Wei, N., and Deng, X. W. (1996) *EMBO J.* **15,** 3732–3743
34. Chattopadhyay, S., Puente, P., Deng X. W., and Wei, N. (1998b) *Plant J* **15,** 69–77
35. Yadav, V., Kundu, S., Chattopadhyay, D., Negi, P., Wei, N., Deng, X. W., and Chattopadhyay, S. (2002) *Plant J* **31,** 741–753
36. Gilmartin, P. M., Memelink, J., Hiratsuka, K., Kay, S. A., and Chua, N. H. (1992) *Plant Cell* **4,** 839–849
37. Schindler, U., Terzaghi, W., Beckmann, H., Kadesch, T., and Cashmore, A. R. (1992) *EMBO J.* **11,** 1275–1289
38. Menkens, A. E., Schindler, U., and Cashmore, A. R. (1995) *Trends Biochem. Sci.* **20,** 506–510
39. Terzaghi, W. B., Bertekap, R. L., Jr., and Cashmore, A. R. (1997) *Plant J.* **11,** 967–982
40. Boter, M., Ruiz-Rivero, O., Abdeen, A., and Prat, S. (2004) *Genes Dev.* **18,** 1577–1591
41. Lorenzo, O., Chico, J. M., Sanchez-Serrano, J. J., and Solano, R. (2004) *Plant Cell* **16,** 1938–1950
42. Guo, H., Yang, H., Mockler, T. C., and Lin, C. (1998) *Science* **279,** 1360–1363
43. Parks, B. M., and Quail, P. H. (1993) *Plant Cell* **5,** 39–48
44. Steindler, C., Matteucci, A., Sessa, G., Weimar, T., Ohgishi, M., Aoyama, T., Morelli, G., and Ruberti, I. (1999) *Development* **126,** 4235–4245
45. Liu, W., Xu, Z. H., Luo, D., and Xue, H. W. (2003) *Plant J* **36,** 189–202
46. Alonso, J. M., Stepanova, A. N., Leisse, T. J., Kim, C. J., Chen, H., Shinn, and Stevenson, D. K., Zimmerman, J., Barajas, P., Cheuk, R., Gadrinab, C., Heller, C., Jeske, A., Koesema, E., Meyers, C. C., Parker, H., Prednis, L., Ansari, Y., Choy, N., Deen, H., Geralt, M., Hazari, N., Hom, E., Karnes, M., Mulholland, C., Ndubaku, R., Schmidt, I., Guzman, P., Aguilar-Henonin, L., Schmid, M., Weigel, D., Carter, D. E., Marchand, T., Risseeuw, E., Brogden, D., Zeko, A., Crosby, W. L., Berry, C. C., and Ecker, J. R. (2003) *Science* **301,** 653–657
47. Bowler, C., Neuhaus, G., Yamagata, H., and Chua, N. H. (1994) *Cell* **77,** 73–81
48. Barnes, S. A., Quaggio, R. B., Whitelam, G. C., and Chua, N. H. (1996) *Plant J.* **10,** 1155–1161